J|A|C|S
ARTICLES

Published on Web 05/01/2009

Effect of Electronic Structures of Au Clusters Stabilized by Poly(*N*-vinyl-2-pyrrolidone) on Aerobic Oxidation Catalysis

Hironori Tsunoyama,[†] Nobuyuki Ichikuni,[‡] Hidehiro Sakurai,[§] and Tatsuya Tsukuda*[,†,⊥]

Catalysis Research Center, Hokkaido University, Nishi 10, Kita 21, Sapporo 001-0021, Japan, Department of Applied Chemistry and Biotechnology, Graduate School of Engineering, Chiba University, Inage-ku, Chiba 263-8522, Japan, Research Center for Molecular Scale Nanoscience, Institute for Molecular Science, Myodaiji, Okazaki 444-8787, Japan, and CREST, Japan Science and Technology Agency, Kawaguchi, Saitama 332-0012, Japan

Received December 24, 2008; E-mail: tsukuda@cat.hokudai.ac.jp

Abstract: Au clusters smaller than 1.5 nm and stabilized by poly(*N*-vinyl-2-pyrrolidone) (PVP) showed higher activity for aerobic oxidation of alcohol than those of larger size or stabilized by poly(allylamine) (PAA). X-ray photoelectron spectroscopy, Fourier transform infrared spectroscopy of adsorbed CO, and X-ray absorption near edge structure measurements revealed that the catalytically active Au clusters are negatively charged by electron donation from PVP, and the catalytic activity is enhanced with increasing electron density on the Au core. Based on similar observations of Au cluster anions in the gas phase, we propose that electron transfer from the anionic Au cores of Au:PVP into the LUMO (π^*) of O_2 generates superoxo- or peroxo-like species, which plays a key role in the oxidation of alcohol. On the basis of these results, a simple principle is presented for the synthesis of Au oxidation catalysts stabilized by organic molecules.

Introduction

The first report of oxidation catalysis using gold clusters by Haruta et al.[1] caused extensive interest in gold catalysts in both the academic and industrial communities. The Au catalysts are divided into two categories, depending on the focus of research interest; i.e. practical vs model catalysts. For the former, various kinds of supported Au catalysts have been developed with practical objectives, such as to achieve high turnover frequency, selectivity and durability, ease of recovery and to widen the scope of applicable reactions.[2−5] However, the development of heterogeneous catalysts has still relied on a trial-and-error approach, because the controlling factors of the catalysis have not yet been fully understood; the catalytic properties are influenced not only by the individual chemical natures of the Au clusters and support, but also by complex interactions between them.[6−9] In addition, it is not a trivial matter to precisely control the structural parameters of the catalysts; therefore new efforts have been made to overcome such difficulties.[10−12] On the other hand, gas-phase Au clusters have gained much interest as a platform for studying intrinsic chemical properties because the size and charge state can be precisely defined.[13−20] It has been revealed that the activity of Au clusters for CO oxidation is strongly correlated to the electronic structures. However, practical catalysts cannot be realized by a straightforward approach based on such knowledge, because of the difficulty in stabilizing these fragile systems without modification of their intrinsic nature. Therefore, the synthesis of practical Au catalysts with desired activity and selectivity according to rational guiding principles remains a great challenge.

In order to bridge the gap between the two approaches, we initially aimed to develop a simple catalytic system in which

[†] Catalysis Research Center, Hokkaido University.
[‡] Chiba University.
[§] Institute for Molecular Science.
[⊥] CREST.

(1) Haruta, M.; Kobayashi, T.; Sano, H.; Yamada, N. *Chem. Lett.* **1987**, 405.
(2) Haruta, M. *Chem. Rec.* **2003**, *3*, 75.
(3) Hashmi, A. S. K.; Hutchings, G. J. *Angew. Chem., Int. Ed.* **2006**, *45*, 7896.
(4) Corma, A.; Garcia, H. *Chem. Soc. Rev.* **2008**, *37*, 2096.
(5) Pina, C. D.; Falletta, E.; Prati, L.; Rossi, M. *Chem. Soc. Rev.* **2008**, *37*, 2077.
(6) Okumura, M.; Nakamura, S.; Tsubota, S.; Nakamura, T.; Azuma, M.; Haruta, M. *Catal. Lett.* **1998**, *51*, 53.
(7) Yoon, B.; Häkkinen, H.; Landman, U.; Wörz, A. S.; Antonietti, J.-M.; Abbet, S.; Judai, K.; Heiz, U. *Science* **2005**, *307*, 403.
(8) Yan, Z.; Chinta, S.; Mohamed, A. A.; Fackler, J. P., Jr.; Goodman, D. W. *J. Am. Chem. Soc.* **2005**, *127*, 1604.
(9) Sterrer, M.; Yulikov, M.; Fischbach, E.; Heyde, M.; Rust, H.-P.; Pacchioni, G.; Risse, T.; Freund, H.-J. *Angew. Chem., Int. Ed.* **2006**, *45*, 2630.
(10) Tai, Y.; Murakami, J.; Tajiri, K.; Ohashi, F.; Daté, M.; Tsubota, S. *Appl. Catal., A* **2004**, *268*, 183.
(11) Zheng, N.; Stucky, G. D. *J. Am. Chem. Soc.* **2006**, *128*, 14278.
(12) Turner, M.; Golovko, V. B.; Vaughan, O. P. H.; Abdulkin, P.; Berenguer-Murcia, A.; Tikhov, M. S.; Johnson, B. F. G.; Lambert, R. M. *Nature* **2008**, *454*, 981.
(13) Lee, T. H.; Ervin, K. M. *J. Phys. Chem.* **1994**, *98*, 10023.
(14) Wallace, W. T.; Whetten, R. L. *J. Am. Chem. Soc.* **2002**, *124*, 7499.
(15) Socaciu, L. D.; Hagen, J.; Bernhardt, T. M.; Wöste, L.; Heiz, U.; Häkkinen, H.; Landman, U. *J. Am. Chem. Soc.* **2003**, *125*, 10437.
(16) Kim, Y. D.; Fischer, M.; Ganteför, G. *Chem. Phys. Lett.* **2003**, *377*, 170.
(17) Bernhardt, T. M. *Int. J. Mass Spectrom.* **2005**, *243*, 1.
(18) Zhai, H.-J.; Wang, L.-S. *J. Chem. Phys.* **2005**, *122*, 051101.
(19) Fielicke, A.; von Helden, G.; Meijer, G.; Pedersen, D. B.; Simard, B.; Rayner, D. M. *J. Am. Chem. Soc.* **2005**, *127*, 8416.
(20) Fielicke, A.; von Helden, G.; Meijer, G.; Simard, B.; Rayner, D. M. *J. Phys. Chem. B* **2005**, *109*, 23935.

 10.1021/ja810045y CCC: $40.75

Scheme 1. Aerobic Oxidation Catalyzed by Au:PVP (1.3 ± 0.3 nm)

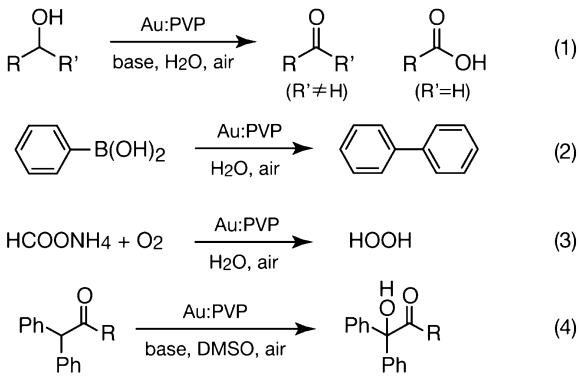

Au clusters are stabilized by catalytically-inert organic molecules, without significant modification of their intrinsic catalytic properties. As an initial target, monodisperse Au clusters weakly stabilized by poly(*N*-vinyl-2-pyrrolidone) (PVP) were selected. In colloidal science, it is well recognized that PVP molecules weakly coordinate to metal clusters through multiple sites in such a way that some portions of the cluster surfaces are exposed for catalysis.[21−27] We have shown that PVP-stabilized Au clusters (Au:PVP) with a core diameter of 1.3 ± 0.3 nm can catalyze various types of aerobic oxidation in water or polar organic solvents as listed in Scheme 1; (1) oxidation of alcohols,[28−31] (2) homocoupling of arylboronic acids,[32,33] (3) in-situ generation of hydrogen peroxide from ammonium formate,[34] and (4) α-hydroxylation of benzylic ketones.[35] These catalytic reactions are valuable for synthetic chemistry and have potential for use in environmentally-benign oxidation processes that utilize molecular oxygen in air as an oxidant.

Size dependence is one of the most intriguing issues of oxidation catalysis using Au:PVP. Figure 1 summarizes the rate constants per unit surface area of Au:PVP with core diameters of 1.0−9.5 nm for the oxidation of *p*-hydroxybenzyl alcohol (*p*-HBA).[28,29,31] Activity appears at a core diameter of ∼5 nm and increases rapidly with decrease in the core size. This trend is reminiscent of the size dependence of the reactivity of gas-phase Au clusters with O_2.[13−17] Previous experimental[16,17] and theoretical[36,37] studies have revealed that cluster anions (Au_n^-) with small even-numbered ($n \leq 14$) and magic ($n = 18, 20$) sizes can generate superoxo-like species via electron transfer to the LUMO of the O_2 molecule. The activation of O_2 has been considered as a key to CO oxidation catalysis using Au clusters. It would be interesting to determine whether such a simple explanation for the gas-phase clusters is also applicable to catalysis with a real system, Au:PVP.

To answer the question, the correlation between the catalytic activity and the electronic structures of Au:PVP was investigated. The charge states of Au cores with different sizes and stabilized by different polymers were probed utilizing X-ray photoelectron spectroscopy (XPS), X-ray absorption near edge structure (XANES), and Fourier transform infrared (FTIR)

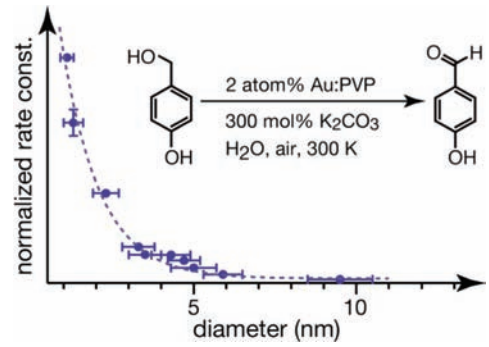

Figure 1. Dependence of catalytic activity on the size of Au:PVP for the oxidation of *p*-HBA (see inset).

spectroscopy of CO molecules[38−41] adsorbed on the Au clusters. The spectroscopic measurements revealed that the active Au clusters are negatively charged by electron donation from PVP and we proposed that a superoxo-like species generated on the negatively charged Au clusters plays a key role in the oxidation of alcohol. The present investigation demonstrates that PVP not only acts as a stabilizer,[21−27] but also plays a direct role in regulating the electronic structures of the metal clusters to promote the catalysis. This understanding provides a simple guiding principle for the fabrication of active Au catalysts.

Experimental Section

Preparation of PVP-Stabilized Au Clusters (1a−1d). Details of the preparation of Au:PVP clusters (**1a**−**1d**) have been described elsewhere.[28,29,31,32] The concentrations and quantities of reagents used are given in Table 1. Briefly, clusters **1a** (ref 31) and **1b** (ref 32) were obtained by mixing aqueous solutions of $HAuCl_4$/PVP (averaged molecular weight $M_W = 40$ kDa) and a strong reducing agent ($NaBH_4$) at 273 K using a micromixer (SIMM-V2, IMM GmbH) and an Erlenmeyer flask, respectively. Clusters **1c** and **1d** were prepared by growing **1b** as a seed (seed-mediated growth method).[28,29] A mixture of hydrosol of **1b** and an aqueous solution of PVP was deaerated by freeze−pump−thaw (FPT) cycles and purged with Ar. The deaerated solutions of $HAuCl_4$ and Na_2SO_3 were then sequentially added to the mixed solution. The final concentration ratios of PVP monomer units to gold, [PVP]/[Au], were 40 and 100 for **1a** and **1b**−**1d**, respectively (Table 1). Clusters **1a**−**1d** were stored in powder form after ultrafiltration of the hydrosol using a membrane filter with a molecular weight cutoff (MWCO) of 10 kDa.

Preparation of PAA-Stabilized Au Clusters (2). As a reference to examine the effect of the polymer, Au clusters stabilized by poly(allylamine) (PAA; $\bar{M}_W = 17{,}000$) (**2**) were prepared by a procedure similar to that used for **1b**. PAA (285 mg, 100 eq. mol

(21) Teranishi, T.; Miyake, M. *Chem. Mater.* **1998**, *10*, 594.
(22) Teranishi, T.; Kiyokawa, I.; Miyake, M. *Avd. Mater.* **1998**, *10*, 596.
(23) Li, Y.; El-Sayed, M. A. *J. Phys. Chem. B* **2001**, *105*, 8938.
(24) Yonezawa, T.; Toshima, N. In *Advanced Functional Molecules and Polymers*; Nalwa, H. S., Ed.; OPA: Amsterdam, 2001; Vol. 2, p 65.
(25) Toshima, N. In *Nanoscale Materials*; Liz-Marzan, L. M.; Kamat, P. V., Eds.; Kuwer Academic Publishers, Boston/Dordrecht/London, 2003; p 79.
(26) Narayanan, R.; El-Sayed, M. A. *J. Phys. Chem. B* **2005**, *109*, 12663.
(27) Zhang, Y.; Grass, M. E.; Kuhn, J. N.; Tao, F.; Habas, S. E.; Huang, W.; Yang, P.; Somorjai, G. A. *J. Am. Chem. Soc.* **2008**, *130*, 5868.
(28) Tsunoyama, H.; Sakurai, H.; Negishi, Y.; Tsukuda, T. *J. Am. Chem. Soc.* **2005**, *127*, 9374.
(29) Tsunoyama, H.; Sakurai, H.; Tsukuda, T. *Chem. Phys. Lett.* **2006**, *429*, 528.
(30) Tsunoyama, H.; Tsukuda, T.; Sakurai, H. *Chem. Lett.* **2007**, *36*, 212.
(31) Tsunoyama, H.; Ichikuni, N.; Tsukuda, T. *Langmuir* **2008**, *24*, 11327.
(32) Tsunoyama, H.; Sakurai, H.; Ichikuni, N.; Negishi, Y.; Tsukuda, T. *Langmuir* **2004**, *20*, 11293.
(33) Sakurai, H.; Tsunoyama, H.; Tsukuda, T. *J. Organomet. Chem.* **2007**, *692*, 368.
(34) Sakurai, H.; Tsunoyama, H.; Tsukuda, T. *Trans. Mater. Res. Soc. Jpn.* **2006**, *31*, 521.
(35) Sakurai, H.; Kamiya, I.; Kitahara, H.; Tsunoyama, H.; Tsukuda, T. *Synlett* **2009**, 245.
(36) Yoon, B.; Häkkinen, H.; Landman, U. *J. Phys. Chem. A* **2003**, *107*, 4066.
(37) Molina, L. M.; Hammer, B. *J. Chem. Phys.* **2005**, *123*, 161104.

Table 1. Reagent Specifications for the Preparation of **1a**-**1d**

	PVP		$HAuCl_4$		**1b**		$NaBH_4$		Na_2SO_3		
sample	conc.[a,b]	vol.[c]	conc.[b]	vol.[c]	conc.[d]	vol.[c]	conc.[b]	vol.[c]	conc.[b]	vol.[c]	[PVP]/[Au][f]
1a	300	20.0	30	10.0	−		50[e]	30.0	−		40
1b	104	48.3	30	1.67	−		100	5.0	−		100
1c	100	90.0	30	3.0	1	90.0	−		90	3.0	100
1d	240	62.5	30	5.0	1	50.0	−		90	5.0	100

[a] In monomer unit. [b] mM. [c] mL. [d] Atomic concentration of Au in mM. [e] Mixed with PVP at a concentration of 200 mM. [f] Final concentration ratio.

Chart 1. Structure of Polymers Used for Clusters **1** and **2**

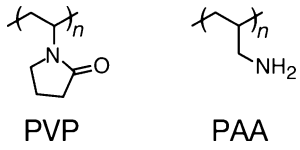

in monomer unit) was added to an aqueous solution of $HAuCl_4$ (1 mM, 50 mL) and stirred for 30 min in a methanol bath at 273 K. An aqueous solution of $NaBH_4$ (100 mM, 5 mL), cooled in an ice bath, was then quickly added to the mixture with vigorous stirring. The reaction mixture was further stirred for 1 h at 273 K. The hydrosol was then deionized by ultrafiltration using a membrane filter (MWCO 5 kDa) to obtain cluster **2**.

Characterization of Au Clusters. Au core size was determined by transmission electron microscopy (TEM; JEM-2000FX, JEOL) and powder X-ray diffraction (XRD; RINT-2000/PC, Rigaku). TEM images were obtained at 200 kV with a typical magnification of 200,000. XRD patterns were recorded using Cu Kα radiation under operation at 40 kV and 40 mA.

UV−vis spectra (V-670, Jasco) of hydrosols **1a**−**1d** and **2** were measured at a given concentration of Au (0.2 mM).

FTIR spectra (FTIR-4200, Jasco) of CO molecules adsorbed on the Au cores of **1a**−**1d** were recorded with a resolution of 4 cm^{-1}. Clusters **1a** (81 mg) and **1b**−**1d** (180 mg) were dispersed in CH_2Cl_2 (3 mL) so that the UV−vis spectra of the organosols exhibited comparable areal intensities. The organosols were placed in a septum-sealed, two-neck flask, deaerated using FPT cycles, and purged with atmospheric pressure of CO. After stirring for 15 min at 295 ± 1 K, the **1a**−**1d** organosols were transferred into a cell (CaF_2 window, 0.5 mm thickness) through a 1/16 in. PTFE tube, and the FTIR spectra were recorded in transmission mode by averaging 20 times. Background spectra were recorded after degassing of CO by several FPT cycles and purging with Ar.

X-ray photoelectron (XP) spectra (JPC-9010MC, JEOL) of the Au 4f core level were measured using a Mg $K\alpha_{1,2}$ X-ray source (photon energy = 1253.6 eV). In order to increase the *S*/*N* ratio of the spectra, each amount of PVP and PAA was reduced to ∼50% by ultrafiltration with a membrane filter (MWCO 50 kDa). The samples were dried for more than 24 h using a lyophilizer (FDU-2200, Eyela). The spectra for **1a**−**1d** and **2** were calibrated using the C1s peaks of PVP and PAA, respectively, as internal standards.[42] In order to study the effect of electrification of the sample on the spectral shift, the spectra were compared with those measured using a different apparatus with a neutralizer (ESCALAB220iXL, VG Scientific). The positions of the Au $4f_{7/2}$ peaks for **1a**−**1d** were almost the same (±0.1 eV) with or without the neutralizer.

X-ray absorption near edge structure (XANES) spectra at the Au L_3 edge were recorded using the BL-12C beamline at the Photon Factory of the Institute for Material Structure Science (PF-IMSS, KEK, No. 2008G687). Synchrotron radiation emitted from the 2.5 GeV storage ring was monochromatized using a Si(111) double-crystal monochromator. Powder samples were pressed into self-supporting disks and sealed into polyethylene bags in a glovebox purged with nitrogen. All the spectra were recorded at room temperature in transmission mode using ion chambers for detection.

General Procedure for Aerobic Oxidation of Alcohol. Aerobic oxidation of *p*-hydroxybenzyl alcohol (*p*-HBA) (eq 5) was carried out in a temperature-controlled personal organic synthesizer (PPS-2510, Eyela) under an air atmosphere. *p*-HBA (31.0 mg, 0.25 mmol) and K_2CO_3 (103.7 mg, 0.75 mmol) were dissolved in H_2O (10 mL) placed in a test tube (ϕ = 30 mm) by sonication for 2 min. The hydrosol of the Au clusters (1 mM, 5 mL) was added to this mixture;[43] the Au content was 2 at % with respect to the substrate. For **1a**, 33.3 mg of PVP was added to the hydrosol to maintain a constant concentration of PVP for **1b**−**1d**. The reaction mixture was stirred vigorously (1300 rpm) at 300 ± 0.5 K, and an aliquot (1 mL) was sampled every hour. After quenching the reaction with 1 M HCl (0.4 mL), the products were extracted three times with AcOEt (10 mL). Combined organic layers were dried over Na_2SO_4 and diluted to 50 mL before gas chromatography (GC) analysis. The ^1H NMR (ECX-400, JEOL) and GC analysis (GC-2014, Shimadzu) revealed that *p*-hydroxybenzaldehyde was the unique product (eq 5). The absolute yield of the product was determined by GC using the external standard method.

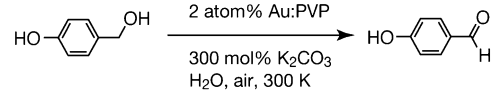

(5)

Results and Discussion

Size Distribution and Catalytic Activity. Representative TEM images of **1a**−**1d** and **2** are shown in Figure 2. The Au core diameters of more than 300 particles were measured and plotted as the histograms in Figure 2. Table 2 summarizes the average diameters determined from the histograms; the results for **1a**−**1d** were in good agreement with those reported in our previous studies.[29,31] However, it is nontrivial to differentiate the sizes of **1a**, **1b**, and **2** from the TEM images, due to the inherent difficulty of imaging metal clusters smaller than 2 nm using TEM.[44] Thus, the average diameters of Au crystallites were also evaluated by applying the Scherrer formula to the diffraction peaks from the Au(111) planes[21,31] after subtracting the contribution of PVP (Figures 3 and S1−S3).[45] XRD analysis confirmed that the average diameter decreased in the order of **2** ≈ **1b** > **1a**, which corresponds to the TEM results (Table 2). Figure 4 shows the UV−vis absorption spectra of **1a**−**1d** and **2**; the surface plasmon band at ∼520 nm is less enhanced for clusters **1a**, **1b** and **2**, which is consistent with the results in Table 2.

In order to evaluate the catalytic activities of **1a**−**1d** and **2** for eq 5, time-evolution of conversion, *C*, was monitored from the measured yield of product. The term $-\ln(1 - C)$ increased linearly with the reaction time for all the clusters (Figure S4),[45] indicating that the reaction is first order with respect to *p*-HBA. The rate constant was determined from the slope of the

(38) Bradley, J. S. "Chapter 6. The Chemistry of Transition Metal Colloids" in *Clusters and Colloids: From theory to applications*; Schmid, G., Ed.; VCH New York, 1994.
(39) Wang, Y.; Toshima, N. *J. Phys. Chem. B* **1997**, *101*, 5301.
(40) Chen, M.; Goodman, D. W. *Acc. Chem. Res.* **2006**, *39*, 739.
(41) Freund, H.-J. *Catal. Today* **2006**, *117*, 6.

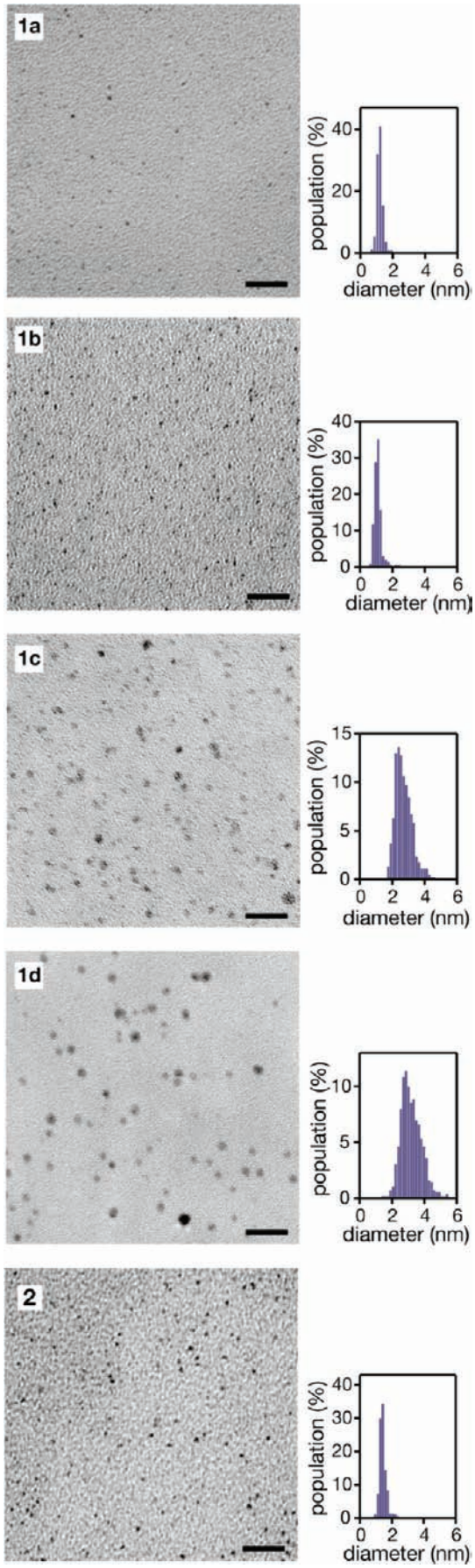

Figure 2. Representative TEM images and size distributions of **1a**−**1d** and **2**. The scale bars represent 20 nm.

Table 2. Average Cluster Size and Catalytic Activity

	1a	1b	1c	1d	2
d_{TEM} (nm)[a]	1.1 ± 0.2	1.2 ± 0.2	2.6 ± 0.6	3.1 ± 0.8	1.4 ± 0.4
d_{XRD} (nm)[b]	0.9	1.0	−	−	1.0
TOF (mol·(surf. atom)$^{-1}$·h^{-1})[c]	33	22	13	4.4	2.6

[a] Average diameter obtained from TEM images. [b] Crystallite size estimated from the Au(111) peak using the Scherrer formula. [c] Turnover frequency for eq 5 at [*p*-HBA] = 16.6 mM and [Au] = 0.33 mM.[45]

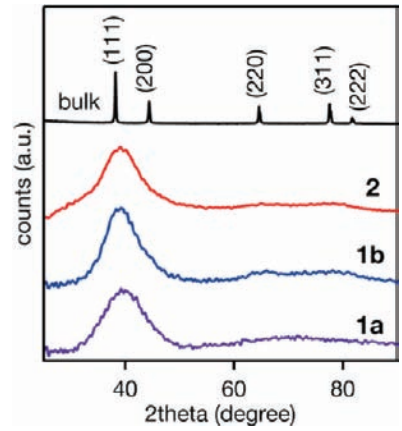

Figure 3. Powder XRD patterns of **1a**, **1b**, and **2** after subtracting the contribution of PVP.

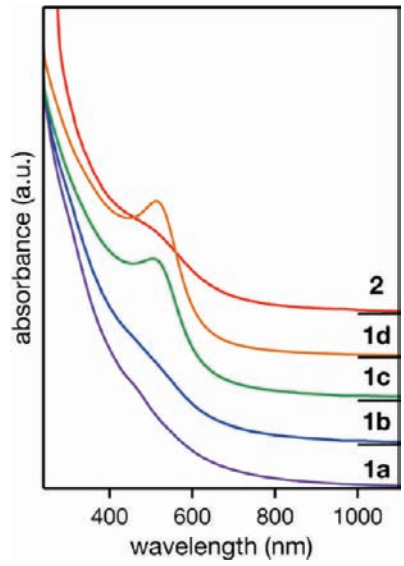

Figure 4. UV−vis absorption spectra of **1a**−**1d** and **2**.

$-\ln(1 - C)$ plot as a function of time.[45] Turnover frequency (TOF) normalized by the number of the surface atoms of the Au cores was calculated from the rate constant thus obtained for concentrations of [*p*-HBA] = 16.6 mM and [Au] = 0.33 mM.[45] The TOF values listed in Table 2 demonstrate two important results. First, the catalytic activity of Au:PVP decreases rapidly with increase in the core size. Second, comparison of **1b** and **2** shows that the activity of Au clusters is much higher when stabilized by PVP than by PAA.

Effect of Cluster Size on Electronic Structures of Au:PVP. It is known that CO molecules are adsorbed atop of Au atoms of clusters and surfaces. Thus, the stretching frequency of adsorbed CO (ν_{CO}) mainly reflects the electron density on the

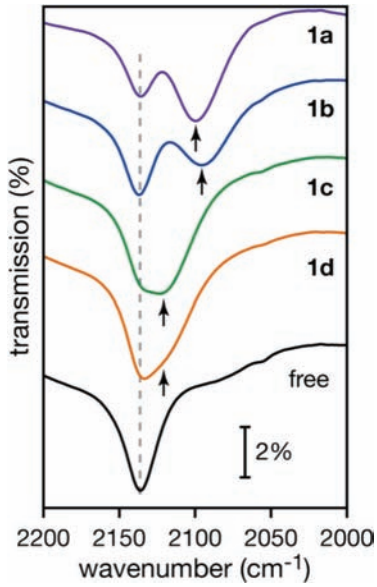

Figure 5. FTIR spectra of ^{12}CO molecules adsorbed on **1a**−**1d**.

adsorption sites; the ν_{CO} is red- and blue-shifted with respect to that of free CO when CO is adsorbed on anionic and cationic Au sites, respectively.[7,9,19,20,40,41] Thus, we first examined the electronic structures of Au cores of Au:PVP using FTIR spectroscopy of adsorbed CO. Figure 5 shows the FTIR spectra of ^{12}CO molecules in CH_2Cl_2 in the presence of **1a**−**1d** at the [PVP]/[Au] ratios of 100. In addition to the peak of CO dissolved in the solvent (2137 cm^{-1}), new peaks are clearly observed at ∼2100 cm^{-1} for **1a** and **1b**, and humps are discernible at ∼2120 cm^{-1} for **1c** and **1d**. These peaks and humps indicated by arrows are assigned to CO molecules adsorbed on the Au core based on the following observations: (1) they were not observed in the absence of Au:PVP, (2) they decay more slowly than that of free CO during evacuation and disappear in the absence of CO. The ν_{CO} values for **1c** and **1d** are comparable to those for the bulk gold reported in literature (2110−2120 cm^{-1}).[46−49] This result indicates that the charge states of Au cores of **1c** and **1d** are similar to that of the bulk gold. In contrast, the ν_{CO} values for **1a** (2099 cm^{-1}) and **1b** (2095 cm^{-1}) are significantly red-shifted from those of **1c** and **1d**. We conclude that the Au cores of **1a** and **1b** are negatively charged according to the criterion that the ν_{CO} values lower than those for bulk Au, especially in the range of <2080 cm^{-1}, have been assigned to CO adsorbed on negatively charged Au sites.[7,40,41] However, it is noticeable that the ν_{CO} values of **1a** and **1b** are not as low as those previously reported for negatively charged Au clusters; (1) ^{12}CO on small Au clusters anchored on color centers of an MgO surface exhibited a broad peak at ∼2070 cm^{-1};[41] (2) ^{13}CO on Au_8 soft-landed on a defect-rich MgO(100) showed the peaks in the range of 2055−2049 cm^{-1}, which correspond to 2102−2096 cm^{-1} for ^{12}CO;[7] (3) ^{12}CO on isolated Au cluster anion (Au_n; $n = 3-14$) exhibited a peak in the range of 2078−1995 cm^{-1}.[20] The smaller red-shift for **1a** and **1b** is attributable to smaller amount of electronic charge deposited on the Au cores and/or larger size of the Au cores.

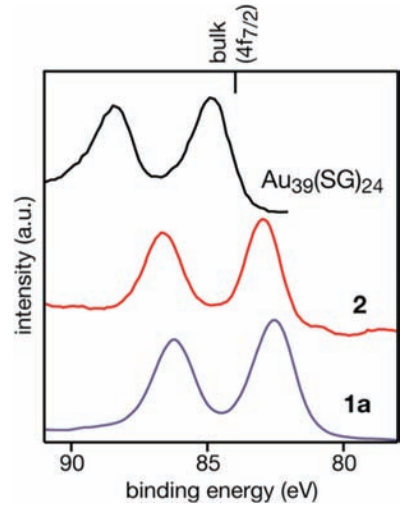

Figure 6. XP spectra of **1a**, **2**, and $Au_{39}(SG)_{24}$ in the vicinity of Au 4f. The spectrum of $Au_{39}(SG)_{24}$ is taken from ref 53.

We next studied the size dependence of the electronic structures of **1a**−**1d** using XPS and XANES. The binding energies (BEs) of Au $4f_{7/2}$ for **1a** and **1b** are determined as 82.7 eV from the XP spectrum (Figure S5), which are significantly smaller than that of bulk gold (84.0 eV). Au $4f_{7/2}$ BEs smaller than that of bulk gold have been reported for micrometer-sized Au:PVP (83.7 eV)[42] and Ni doped Au clusters protected by alkanethiolate (82.0 eV),[50] and were ascribed to the negative charge states of Au. Thus, the XPS measurement supports the above conclusion that *the Au cores of **1a** and **1b** are negatively charged*. The increase in the electron density in the Au cores of **1a** and **1b** is also confirmed by XANES spectra (Figure S6). The intensity of the white line (WL) at the Au L_3 edge (ca. 11923 eV), which corresponds to the transition from $2p_{3/2}$ to mainly $5d_{5/2}$ above the Fermi level, is smaller for **1a** and **1b** than bulk gold. This result indicates that the densities of d-holes of the Au cores of **1a** and **1b** are smaller than that of bulk gold (0.4 e).[51] However, contrary to expectations from the results of Figure 5, the XPS and XANES revealed that the Au cores are negatively charged regardless of the size; the Au $4f_{7/2}$ binding energies of for **1c** and **1d** were also 82.7 eV (Figure S5) and the intensity of the WL of **1c** is smaller than that of the bulk gold (Figure S6).[45] Therefore, these results indicate that *smaller Au:PVP clusters have the ability to donate more electronic charge to CO than larger clusters, although the Au cores are negatively charged regardless of their size.* Similar size-dependent behavior has been observed for Au cluster anions in the gas phase.[20] The ν_{CO} of $Au_n(CO)^-$ is gradually red-shifted from 2078 to 1995 cm^{-1} with decreasing cluster size from $n =$ 14 to 2, which indicates more efficient electron transfer to CO from smaller Au cluster anions. More efficient electron transfer from smaller Au:PVP to CO is probably ascribed to high-lying orbitals that accommodate excess electric charge since the LUMO levels of free Au clusters become higher in energy with decrease in size.[52]

Effect of PVP on Electronic Structures of Au:PVP. What is a source of the excess electronic charge of the Au cores of Au:PVP? In order to address the question, we studied the effect

(42) Jiang, P.; Zhou, J.-J.; Li, R.; Gao, Y.; Sun, T.-L.; Zhao, X.-W.; Xiang, Y.-J.; Xie, S.-S. *J. Nanopart. Res.* **2006**, *8*, 927.
(43) The concentration was normalized to keep areal intensity in the optical absorption spectrum constant.
(44) Pyrz, W. D.; Buttrey, D. J. *Langmuir* **2008**, *24*, 11350.
(45) See supporting information.
(46) Ruggiero, C.; Hollins, P. *Surf. Sci.* **1997**, *377*−*379*, 583.
(47) Jugnet, Y.; Cadete Santos Aires, F. J.; Deranlot, C.; Piccolo, L.; Bertolini, J. C. *Surf. Sci.* **2002**, *521*, L639.
(48) Kim, J.; Samano, E.; Koel, B. E. *J. Phys. Chem. B* **2006**, *110*, 17512.

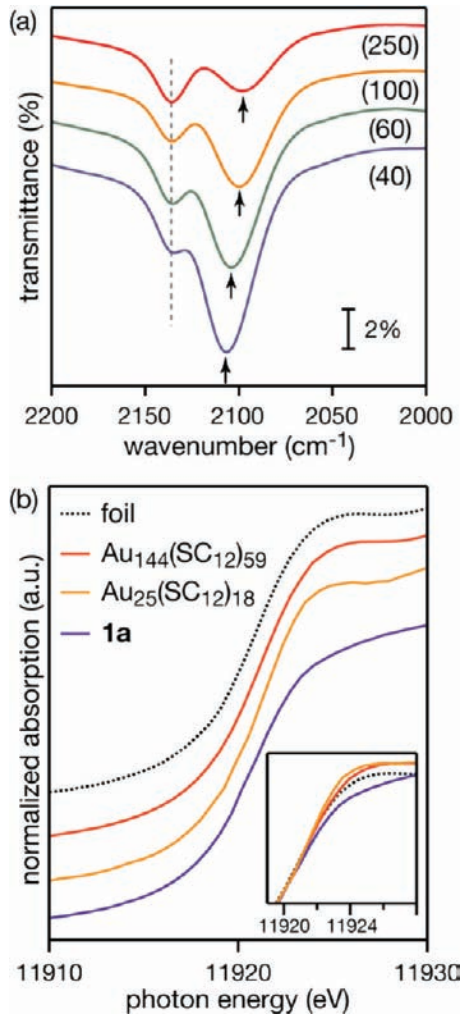

Figure 7. (a) FTIR spectra of ^{12}CO adsorbed on **1a** with various PVP concentrations. The values in parentheses indicate the concentration ratios of PVP monomer units to Au. (b) Au L_3 edge XANES spectra of **1a**, $Au_{25}(SC_{12})_{18}$ and $Au_{144}(SC_{12})_{59}$.

of the organic stabilizers on the electronic structures of the Au cores. Figure 6 shows the XP spectra of **1a** and **2** of which Au clusters with comparable sizes (Table 2) are stabilized by PVP and PAA (Chart 1). As a comparison, the XP spectrum of Au_{39} clusters protected by glutathionate (SG)[53] is also presented in Figure 6, although they do not show any catalytic activity due to complete protection of the Au cores. The Au $4f_{7/2}$ BEs of **1a**, **2** and $Au_{39}(SG)_{24}$ are determined to be 82.7, 83.4, and 84.9 eV,[53] respectively. These BEs indicate that electronic charge is donated to the Au core from PVP and PAA, whereas that of the Au core is abstracted by SG. Therefore, the excess electronic charge on the Au cores of Au:PVP comes from PVP. Electron transfer from PVP to small Pt clusters has also been reported.[54,55]

In order to further confirm the electron donation from PVP to Au clusters, we studied the charge states of Au core as a function of PVP concentration. Figure 7 shows the FTIR spectra of ^{12}CO adsorbed on the Au core of **1a** dispersed in CH_2Cl_2

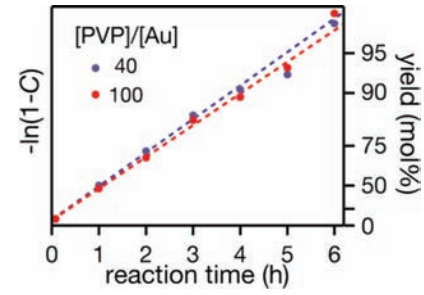

Figure 8. Time course of conversion (C) for eq 5 catalyzed by **1a** under different PVP concentrations; [PVP]/[Au] = 40 (blue) and 100 (red).

containing different amounts of PVP.[56] The relative population of adsorbed CO, with respect to the free CO dissolved in the solvent, gradually decreases with increase of the PVP concentration. This trend indicates that PVP is bound more strongly than CO and that the ν_{CO} value monitors the charge states of the Au sites uncoordinated by PVP. The ν_{CO} value for adsorbed ^{12}CO is monotonically red-shifted from 2107 cm^{-1} to 2098 cm^{-1} with increase in the [PVP]/[Au] ratios from 40 to 250. The peak for adsorbed ^{13}CO is also red-shifted from 2060 to 2050 cm^{-1} with increasing PVP concentration (Figure S7). The result indicates that additional PVP does donate more electronic charge to the Au cores of **1a**, which provides crucial evidence that *PVP not only acts as a stabilizer but also plays a direct role in regulating the electronic structures*[42,54,55] *of the Au clusters*. The essential role of PVP in the electron donation to Au clusters was also demonstrated by XANES spectra of **1a**, dodecanthiolate ($C_{12}S$)-protected Au clusters, $Au_{25}(SC_{12})_{18}$ (ref 57) and $Au_{144}(SC_{12})_{59}$ (ref 58) (Figure 7b). The XANES spectra of $Au_{25}(SC_{12})_{18}$ and $Au_{144}(SC_{12})_{59}$ indicate that densities of d-holes of the Au cores protected by thiolates are larger than the bulk regardless of the core size. Thus, decrease in the densities of d-holes in **1a** is not due to effect of the Au core size[59] but to the interaction with organic stabilizers,[60] i.e., electron donation from PVP.[54,55]

The above conclusion is supported by a recent theoretical calculation by Okumura et al.[61] They studied the geometrical and electronic structures of the complex formed by icosahedral Au_{13} and four molecules of ethylpyrrolidone (EP), which models the PVP monomer unit. It was found that the C=O groups of the EP molecules coordinate on top of the Au atoms of the Au_{13} core. A Mulliken charge analysis revealed that the Au_{13} core was negatively charged due to the coordination of EP molecules.

(49) Chen, M.; Cai, Y.; Yan, Z.; Goodman, D. W. *J. Am. Chem. Soc.* **2006**, *128*, 6341.
(50) Auten, B. J.; Hahn, B. P.; Vijayaraghavan, G.; Stevenson, K. J.; Chandler, B. D. *J. Phys. Chem. C* **2008**, *112*, 5365.
(51) Mattheiss, L. F.; Dietz, R. E. *Phys. Rev. B* **1980**, *22*, 1663.
(52) Taylor, K. J.; Pettiette-Hall, C. L.; Cheshnovsky, O.; Smalley, R. E. *J. Chem. Phys.* **1992**, *96*, 3319.
(53) Negishi, Y.; Nobusada, K.; Tsukuda, T. *J. Am. Chem. Soc.* **2005**, *127*, 5261.
(54) Borodko, Y.; Habas, S. E.; Koebel, M.; Yang, P.; Frei, H.; Somorjai, G. A. *J. Phys. Chem. B* **2006**, *110*, 23052.
(55) Qiu, L.; Liu, F.; Zhao, L.; Yang, W.; Yao, J. *Langmuir* **2006**, *22*, 4480.
(56) FTIR spectra of **2** could not be obtained because they were not dissolved in the solvents applicable to the measurement (CH_2Cl_2, $CHCl_3$, CH_3CN).
(57) Negishi, Y.; Chaki, N. K.; Shichibu, Y.; Whetten, R. L.; Tsukuda, T. *J. Am. Chem. Soc.* **2007**, *129*, 11322.
(58) Chaki, N. K.; Negishi, Y.; Tsunoyama, H.; Shichibu, Y.; Tsukuda, T. *J. Am. Chem. Soc.* **2008**, *130*, 8608.
(59) van Bokhoven, J. A.; Miller, J. T. *J. Phys. Chem. C* **2007**, *111*, 9245.
(60) Zhang, P.; Sham, T. K. *Appl. Phys. Lett.* **2002**, *81*, 736.
(61) Okumura, M.; Kitagawa, Y.; Kawakami, T.; Haruta, M. *Chem. Phys. Lett.* **2008**, *459*, 133.
(62) The activity of **1b** is lower than **1a** although the ν_{CO} value for **1b** is red-shifted to that of **1a** (Figure 5). This is probably because the population of available sites for catalysis is lower in **1b** than in **1a**.

Chart 2. Mechanism for the Activation of Molecular Oxygen by Au:PVP

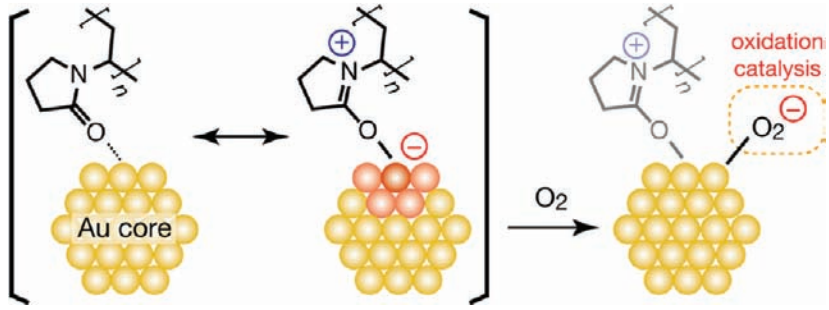

Correlation between Electronic Structures and Oxidation Catalysis. Table 2 summarizes the TOF of Au clusters for aerobic oxidation of *p*-HBA (eq 5). The following correlations between the electronic structures and the oxidation activity were observed.

(1) Smaller Au:PVP clusters (**1a**, **1b**) that can donate more electronic charge to CO molecules exhibit higher activity toward aerobic oxidation than larger clusters (**1c**, **1d**).

(2) When the [PVP]/[Au] ratio increases from 40 to 100 in the **1a** organosol, the areas of coordination sites for CO are significantly decreased as shown in Figure 7. Contrary to expectations from decrease in the area available for catalysis, the activity of **1a** for eq 5 remains unchanged, as shown in Figure 8. This result can be explained in that the decrease of the cluster surface area available for catalysis is compensated by the enhancement of activity per unit surface area by the donation of more electronic charge from PVP.

(3) The charge state of Au clusters stabilized by PAA (**2**) is less negative than that by **1b**, and the activity for oxidation is much lower than that of **1b**, despite the comparable core size (Figure 6 and Table 2). This implies that the lower reactivity of **2** is due to the lower electron-donating ability of PAA, although the possibility that the surface areas available for catalysis are smaller for **2** than for **1b** is not totally excluded.

All of these correlations indicate that *the catalytic activity of small (<2 nm) Au:PVP for aerobic oxidations is enhanced by an increase in the amount of negative charge on the Au core.*[62] This provides an empirical rule for the synthesis of active Au catalysts; more electronic charge should be deposited into high-lying orbitals of small Au clusters by doping with electropositive elements or by interaction with nucleophilic sites of stabilizing molecules. As anticipated, doping of a small amount (<10%) of electropositive Ag into Au:PVP caused the Au site to become more negative and enhanced the catalytic activity.[63]

Oxidation Mechanism. How can the higher catalytic activity of small Au:PVP with more anionic nature be explained? A similar correlation was observed in the gas-phase Au clusters; smaller cluster anions (Au_n^-) exhibit higher reactivity toward O_2 than larger cationic clusters. This trend has been explained in terms of partial electron transfer from Au_n^- to the LUMO (π^*) of O_2. The generation of superoxo-like species on free Au clusters has been evidenced by photoelectron spectroscopy.[16] On the basis of the similarities, we propose that the activation of O_2 by anionic Au cores is also the key step for aerobic oxidation catalyzed by Au:PVP. Chart 2 schematically depicts the activation of O_2 by Au:PVP, in which superoxo- or peroxo-like species are formed on the anionic Au clusters by partial electron transfer.[64] This activation mechanism is also supported by a density functional theory (DFT) study on the complex formed between $Au_{13}(EP)_4$ and O_2; the excess electronic charge of the Au_{13} core is transferred to the adsorbed O_2.[61] This intermediate species then abstracts a β-hydrogen atom from the alcohol to generate the corresponding aldehydes or ketones.

The role of molecular oxygen in the aerobic oxidation of alcohol is different between Au:PVP and Pd catalysts.[65−68] Kaneda and co-workers proposed that oxidation by Pd clusters proceeds via oxidative addition of alcohol onto the Pd(0) surface, followed by β-hydride elimination from the alkoxide to generate palladium-hydride species.[65] The role of O_2 in this catalytic system is to eliminate the hydride species and regenerate Pd(0). In the case of Au:PVP, the superoxo- or peroxo-like species generated on the cluster surface eliminates the β-hydrogen of the alcohol. Such a difference in the reaction mechanism may explain the difference in the activation energies for oxidation of *p*-HBA (eq 5); 20 and 33 kJ mol^{-1} for Au:PVP (**1b**) and Pd:PVP (2.2 $\pm$ 0.4 nm), respectively.[28] As a result, the Au catalysts can catalyze the oxidation of alcohols under milder conditions than the Pd systems which require higher temperature and O_2 pressure.

Finally, we point out the possibility that activated oxygen species on small clusters plays an essential role in other size-specific reactions of Au clusters. We have previously reported that only small Au:PVP can be extracted into the organic phase by reaction with alkanethiols under aerobic conditions.[69,70] This reaction does not proceed under anaerobic conditions. Involvement of molecular oxygen has also been reported in the ligand exchange of phosphine-protected Au clusters with thiols.[71] Ionita et al.[71] proposed that a superoxo-type species abstracts a hydrogen atom from the incoming thiol to form thiolates on the cluster surface. We believe that a similar

(63) Chaki, N. K.; Tsunoyama, H.; Negishi, Y.; Sakurai, H.; Tsukuda, T. *J. Phys. Chem. C* **2007**, *111*, 4885.
(64) No spectroscopic evidence for the formation of superoxo- or peroxo-species was obtained by electron spin resonance and IR spectroscopy. However, formation of hydrogen peroxide during the reaction was confirmed by oxidative formation of I_2 from KI.
(65) Mori, K.; Hara, T.; Mizugaki, T.; Ebitani, K.; Kaneda, K. *J. Am. Chem. Soc.* **2004**, *126*, 10657.
(66) Uozumi, Y.; Nakao, R. *Angew. Chem., Int. Ed.* **2003**, *42*, 194.
(67) Muzart, J. *Tetrahedron* **2003**, *59*, 5789.
(68) Sigman, M. S.; Jensen, D. R. *Acc. Chem. Res.* **2006**, *39*, 221.
(69) Tsunoyama, H.; Negishi, Y.; Tsukuda, T. *J. Am. Chem. Soc.* **2006**, *128*, 6036.
(70) Tsunoyama, H.; Nickut, P.; Negishi, Y.; Al-Shamery, K.; Matsumoto, Y.; Tsukuda, T. *J. Phys. Chem. C* **2007**, *111*, 4153.
(71) Ionita, P.; Gilbert, B. C.; Chechik, V. *Angew. Chem., Int. Ed.* **2005**, *44*, 3720.

mechanism plays a role in the thiolation of small Au:PVP; a hydrogen is abstracted by the activated molecular oxygen shown in Chart 2.

Conclusion

Small (1−3 nm) monodisperse Au clusters stabilized by PVP and PAA were prepared, and the correlation between the electronic structures and the catalytic activity for aerobic oxidation of alcohol (eq 5) was studied. PVP-stabilized Au clusters that were smaller than 1.5 nm showed higher activity than those of larger clusters and PAA-stabilized Au clusters. XPS, FTIR spectroscopy of adsorbed CO, and XANES measurements revealed that these catalytically active clusters are negatively charged by electron donation from PVP. This demonstrates that PVP not only acts as a stabilizer but also plays a direct role to regulate the electronic structure of the Au clusters. The catalytic activity of small (<2 nm) Au clusters for aerobic oxidation is enhanced with increasing negative charge on the Au core. This trend corresponds to that observed for small Au cluster anions in the gas phase, which exhibit higher reactivity to O_2 than larger cationic clusters. On the basis of these similarities, we propose that electron transfer from the anionic Au cores of Au:PVP into the LUMO (π^*) of O_2 generates superoxo- or peroxo-like species that plays a key role in oxidation of the alcohol. This work provides a simple principle for the synthesis of aerobic oxidation catalysts based on the electronic structures of Au clusters; more electronic charge should be deposited into the high-lying orbitals of small Au clusters by doping with electropositive elements or by interaction with nucleophilic sites of stabilizing molecules.

Acknowledgment. This work was financially supported by Grants-in-Aid (Grant No. 18064017, Synergy of Elements) from MEXT and CREST program of JST. H.T. was financially supported by a Research Fellowship from the Japan Society for the Promotion of Science for Young Scientists. We thank Profs. N. Toshima (Tokyo University of Science), H. Nagashima, and Y. Motoyama (Kyushu University) for valuable comments and fruitful discussion. The XRD, XPS, and TEM measurements were performed at the open facility in Hokkaido University.

Supporting Information Available: Analysis of XRD patterns, evaluation of TOF, XPS and XANES. This material is available free of charge via the Internet at http://pubs.acs.org.

JA810045Y